DOI: http://dx.doi.org/10.15446/ing.investig.v38n2.67743

Devolatilization of African Palm (*Elaeis guineensis*) Husk studied by TG-MS

Devolatilización del cuesco de palma estudiada por TG-MS

Alberto Albis [1], Ever Ortiz[2], Ismael Piñeres[3], Andrés Suárez[4], and Marley Vanegas[5]

ABSTRACT

Using simultaneous thermogravimetrical analysis coupled with mass spectroscopy, the pyrolysis of African palm husk, using several heat rates and programs was performed. Seven relations of mass/charge were followed of the evolved gas of the pyrolysis process, fitting the kinetics and the mass spectroscopy signals to the distributed activation energy model (DAEM) with different numbers of pseudo-components. Fitting with four pseudo-components proved to be the best for modeling the thermal degradation process. Kinetic parameters were not affected by the heating rate or program employed, which agrees with other reports for similar biomass. Methane, methanol formaldehyde, furfural were successfully fitted to the DAEM model, nevertheless CO_2 and NO_2 were not able to be represented by this model due to its production in secondary reactions in gaseous phase.

Keywords: TG-MS, pyrolysis, African Palm, husk.

RESUMEN

Se estudió la pirólisis del cuesco de palma africana utilizando diferentes programas de calentamiento, recurriendo al uso de la técnica simultánea de análisis termogravimétrico acoplado a espectrometría de masas. En los gases de evolución, se siguieron las intensidades de señal de espectrometría de masas de siete relaciones *m/z*. La cinética de pirólisis de este residuo del procesamiento de aceite de palma se ajustó al modelo de distribución de energías de activación con diferentes números de pseudo-componentes. Los resultados del ajuste mostraron que son necesarios al menos cuatro pseudo-componentes para modelar satisfactoriamente los perfiles termogravimétricos de la pirólisis del cuesco de palma. Se encontró que la velocidad de calentamiento no afecta significativamente los parámetros del modelo cinético, los cuales se encuentran en concordancia con los reportados en la literatura para biomasas similares. Los perfiles de las curvas de intensidad de señal para las relaciones *m/z* seleccionadas se modelaron utilizando los parámetros cinéticos obtenidos del ajuste de los datos termogravimétricos, lográndose resultados satisfactorios para las relaciones *m/z* correspondientes a fragmentos de moléculas como metano, metanol, formaldehído y furfural. La falta de ajuste de las intensidades de señal correspondientes a CO_2 y NO_2 se atribuyó a que la formación de estos compuestos es consecuencia no sólo de la descomposición de la biomasa, sino también a su aparición resultado de reacciones secundarias en fase gaseosa.

Palabras clave: TG-MS, pirólisis, palma africana, cuesco.

Received: September 15th 2017
Accepted: April 16th 2018

Introduction

Among new alternatives implemented in order to reduce CO_2 and NOx emissions produced by internal combustion engines (Rodríguez, Sierens, Verhelst, & Frontela, 2008), biomass becomes a renewable source of energy, that can partially replace the fossil fuels (Perdices, 2009) and reduce the emissions of those gases to the atmosphere (Montiel, 2003). Thermochemical transformation of biomass usually produces solid, liquid and gas fuels that besides the usage for energy production, can be a source of chemical products, heat and energy (Camps Michelena & Marcos Martín, 2008). Pyrolysis and gasification are the thermochemical

[1] Chemical Engineer, Universidad Nacional de Colombia, Colombia. Dr. Sc. Chemistry, Universidad Nacional de Colombia, Colombia. Affiliation: Associate Professor, Universidad del Atlántico, Colombia.
E-mail: albertoalbis@uniatlantico.edu.co.

[2] Lic. Física, Universidad Pedagógica de Colombia, Colombia. M.Sc. Physics, Universidad del Valle, Colombia. Dr.Sc. Physics, Universidad del Valle, Colombia. Affiliation: Titular Professor, Universidad del Atlántico, Colombia. E-mail: everortiz@uniatlantico.edu.co.

[3] Licentiate In Physics, Universidad del Atlántico, Colombia. M.Sc. Physics, Universidad del Atlántico, Colombia. Affiliation: Assistant Professor, Universidad del Atlántico, Colombia. E-mail: ismaelpineres@uniatlantico.edu.co.

[4] Chemical Engineer, Universidad Nacional de Colombia, Colombia. M.Sc. Chemistry, Universidad Nacional de Colombia, Colombia. Dr. Sc. Chemistry, Universidad Nacional de Colombia, Colombia. Affiliation: Titular Professor, Universidad Jorge Tadeo Lozano, Colombia.
E-mail: andresf.suareze@utadeo.edu.co.

[5] Chemical Engineer, Universidad del Atlántico, Colombia. Ph.D. Tecnología, Diversi-ficación, Calidad y Ahorro Energético, Universidad de Oviedo, Spain. Affiliation: Associate Professor, Universidad del Atlántico, Colombia. E-mail: marleyvanegas@uniatlantico.edu.co.

How to cite: Albis, A., Ortiz, E., Piñeres, I., Suárez, A., Vanegas, M. (2018). Devolatilization of African Palm (Elaeis guineensis) Husk studied by TG-MS. Ingeniería e Investigación, 38(2), 9-17.
DOI: 10.15446/ing.investig.v38n2.67743

processes most used at commercial level (Soto, Machado, & López, 2010). Lignocellulosic biomass is the organic substance most abundant on earth; the main sources of those are forest, crops and industrial residues (Abril & Navarro, 2012). This material is constituted by cellulose, hemicellulose and lignin (Abril & Navarro, 2012; Caballero, 1995). For the systematic characterization of biomass pyrolysis, the analysis of the individual components has been performed using several techniques such as thermogravimetrical analysis (TG), thermogravimetrical analysis coupled with gas chromatography (TG-GC), thermogravimetrical analysis coupled with Fourier transform infrared spectroscopy (TG-FTIR) (D. Chen, Liu, Zhang, Chen, & Li, 2015; Gani & Naruse, 2007; Yang, Yan, Chen, Lee, & Zheng, 2007). Usually, in further investigations, interactions between the components of the biomass and the effect of the addition of alkaline minerals (Lv *et al*., 2010), alkaline earths, and metallic salts is studied (Khelfa, Bensakhria, & Weber, 2013).

Pyrolysis behavior of biomass is dependent on biomass composition; therefore, each feedstock should be thermally characterized to set bio-oil production conditions (Wang, Guo, Wang, & Luo, 2011). Husk of African palm tree is one of the most abundant waste lignocellulosic biomass in countries such as Indonesia, Malaysia, and Colombia, as a result of the extraction of palm oil. Several strategies have been implemented to manage palm oil industry solid wastes and other, such as, gasification and pyrolysis are currently under research (Oseghale, Mohamed, & Chikere, 2017). In this work, the devolatilization kinetics of husk of African palm tree and its product distribution are studied. Simultaneous analysis using TG-MS technique was used. Experimental data were fitted to distributed activation energy model (DAEM). Results could be used to scale up pyrolysis reactors using husk of African palm.

Methodology

Materials

African palm husk (*Elaeis guineensis*) was obtained from a local biodiesel plant. Biomass was grinded (particle size < 200 mm) and stored in a desiccator prior to use.

Elemental analysis

For elemental analysis a Thermo Scientific FLASH 2000 CHNS/O Analyzer with a detection limit of 0,01% was used.

TG-MS analysis

Thermogravimetrical analysis was performed in a TA instruments TGA 2950 thermogravimetric analyzer. A Thermostar (Blazer) mass analyzer was coupled to the thermogravimetric balance to analyze the evolved gases. Linear heating rate programs were employed (10 and 100 K/min), and linear heating intercalated with isothermal processes (step transitions). Selected heating rates allowed visualizing any change of mechanism at fast heating, and stair-like heating program allowed capturing more information from TG and MS experiments. Helium (grade 5) was used as purge gas at a constant flow of 100 mL/min. To reduce the effects of heat and mass transfer (Albis, Ortiz, Suárez, & Piñeres, 2013), the weight of the samples were between 2 and 15 mg. The masses of the samples selected for the mass spectroscopy analysis were selected according to preliminary experimentation, where m/Z values between 1 and 120 were followed while the sample is heated at 10 K/min. From here, channels m/z above base line were selected.

Distributed activation energy model (DAEM)

DAEM model uses the assumption that a series of irreversible parallel first order reactions occurs, characterized for a continuous distribution of activation energy that can be represented by a distribution function $D_j(E)$ (N. Chen *et al*., 2016; Cheng *et al*., 2015). This model describes the processes of pyrolysis, where the fraction of unreacted material as function of time is (Várhegyi, 2007):

$$x_j(t) = \int_0^\infty D_j(E)\, X_j(t,E)\, dE \tag{1}$$

Where $X_j(t,E)$ is the solution of the first order kinetics equation that represents the specific activation energy (Açıkalın, 2011), that is represented by Equation (2).

$$-\frac{dX_j(t,E)}{dt} = A_j exp\left(\frac{-E}{RT(t)}\right) x_j(t,E) \tag{2}$$

For each pseudo-component a kinetic equation represented by Equation (1) is assumed. The weight loss rate curve (DTG) is the pondered sum of the individual reaction rates (N. Chen, *et al*., 2016), which are calculated by Equation (3).

$$Y^{calc}(t) = -\sum_{j=1}^{M} c_j \frac{dx_j}{dt} \tag{3}$$

Where x_j is the unreacted fraction of the material represented by the *j*-th kinetic equation, c_j corresponds to the *j*-th reaction contribution of the measured quantity and M is the number of pseudo-components used for the fitting (Albis, *et al*., 2013). Each curve $\frac{dx_j}{dt}$ of Equation (1), can be obtained from Equation (4) as follows.

$$\frac{dx_j(t)}{dt} = \int_0^\infty D_j(E) \frac{dX_j}{dt}(t,E)\, dE \tag{4}$$

Where $D_j(E)$ is a distribution function for the activation energy of the pseucodomponent *j*. In order to use numerical integration techniques, the inferior integration limit of the

right part of the equation has to be changed from E = 0 to E = -∞. Assuming the usual values for the pre exponential factors, obtaining values of E = 0 or E < 0 corresponds to events that occurs below ambient temperature, so, the change of the limit of the equation does not interfere in the value of the integral (Várhegyi, Szabó, & Antal, 2002). Assuming that a Gaussian distribution function, usually employed for this kind of processes (Cheng, *et al.*, 2015; Janković, 2014), with an apparent media activation energy E_{0j} and an standard deviation σ_j can be obtained.

$$x_j(t) = \int_{-\infty}^{\infty} \frac{1}{\sqrt{2\pi}\,\sigma_j} exp\left[-\frac{\left(E - E_{0j}\right)^2}{2\sigma_j^2} \right] X_j(t,E)\,dE \quad (5)$$

Inducing a variable change proposed previously (Janković, 2014), the Gauss—Hermite quadrature and the re-scaling suggested by other authors, such as Donskoi & McElwain (2000),for improving the equation efficiency:

$$x_j(t) = \frac{1}{2\sqrt{\pi}} \sum_{i=1}^{N} w_i \exp\left[0.75\mu_j^{\,2}\right] X_j\left(t,\mu_j\right) d\mu_j \quad (6)$$

Where represents the ponderation values. In this case a re-scaling factor of 0,5 suggested in previous works was used. Also, in in Equation (6), the number of partitions of the Gauss – Hermite quadrature employed were 80 (Várhegyi, *et al.*, 2002).

For the fitting of the curve, a nonlinear least square method was employed, where the experimental and calculated curves looks for minimize the equation:

$$SE = \sqrt{\frac{\sum_{i=1}^{N_k}\left[Y^{obs}(t_i) - Y^{calc}(t_i)\right]^2}{N_k - Np}} \quad (7)$$

Where N_k represents the number of points for the curve evaluated and *Np* is the number of parameters of the model (Abdelouahed, Leveneur, Vernieres-Hassimi, Balland, & Taouk, 2017).

For the determination of the kinetic parameters of the decomposition of palm husk, distributed activation energy model (DAEM) was used. In this study, the pre-exponential factor of the Arhenius equation for each one of the reactions sets or pseudo-components is independent of the heating speed rate. Experimental data was fitted to the model employing between one and four pseudo-components. The fitting of the model was performed using Matlab® software, evaluating Equation (6) under the criteria of minimization of SE from Equation (7).

Results and discussion

Elemental analysis of the sample shows a percentage of nitrogen of 0,71 %, carbon of 43,09 %, hydrogen of 6,83 % and oxygen of 46,65 %. Biomass has higher contents of O and H and a lower C content than those reported for fossil fuels (Demirbas, 2004).

In Figures 1a and 1b, TG and DTG curves are showed for heating rates of 10 and 100 K/min. The curves shows a similar behavior found in previous studies (Idris *et al.*, 2010; Yang *et al.*, 2004), including a similar percentage of char at both heating rates. In Figure 1 a typical displacement to the right of the thermogram with the increase of the heating rates is exhibit (Várhegyi, 2007).

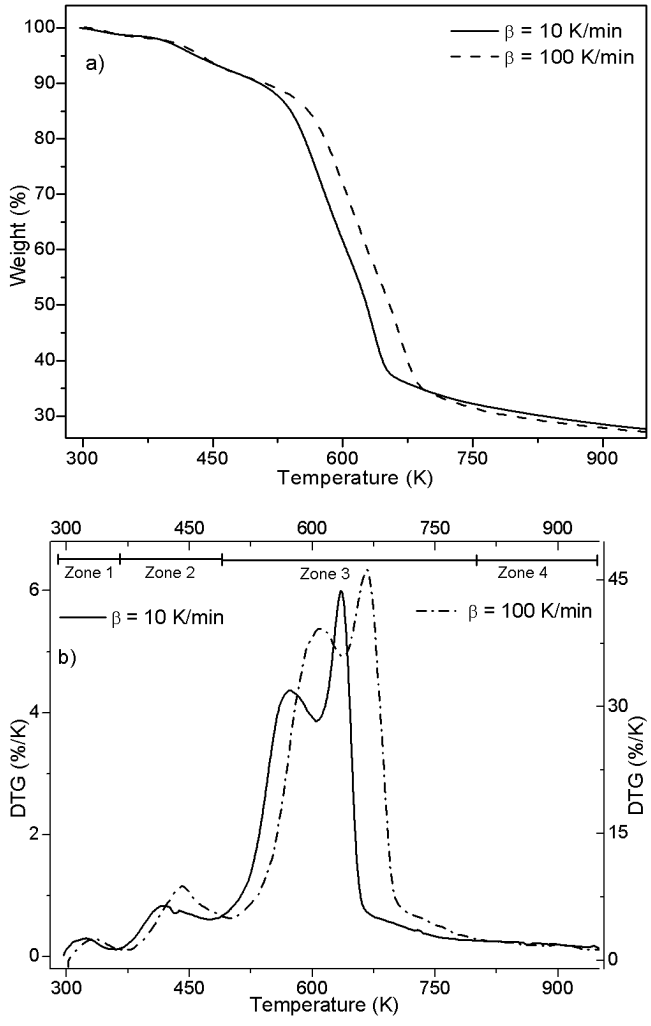

Figure 1. TG and DTG thermogram of palm husk pyrolysis.
Source: Authors

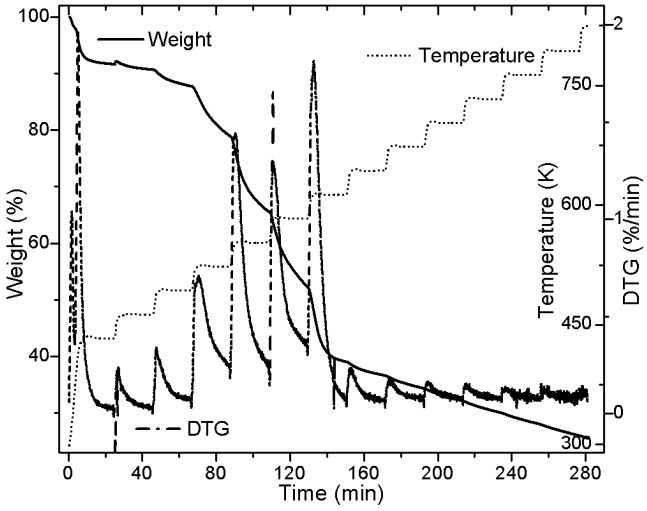

Figure 2. TG and DTG curves for the step heating program of palm kernel shell.
Source: Authors

Thermogram shows a first event that is related with water release (zone 1) (Gottipati & Mishra, 2011), followed by a second event that corresponds to the first thermal decomposition (zone 2), then , the main pyrolytic event is reached with two peaks of similar height (zone 3), and finally, a slow rate decomposition zone (zone 4). Water loss at temperatures below 393 K corresponds to the humidity of the sample, weight loss in zone 2 of the Figure 1b is due to the decomposition of oils and volatile substances in the husk. In the main pyrolytic event, the first peak corresponds to hemicellulose decomposition and the second one represents the disintegration of cellulose. Zone 4 is related to the lignin thermal degradation, which is decomposed in a wide temperature range, and secondary reactions of the thermal decomposition of char residues. Figure 2 shows heating program, TG, and DTG thermograms for the palm husk using the stair function program. This program allows to gather information in case of parallel reactions, like described by DAEM model.

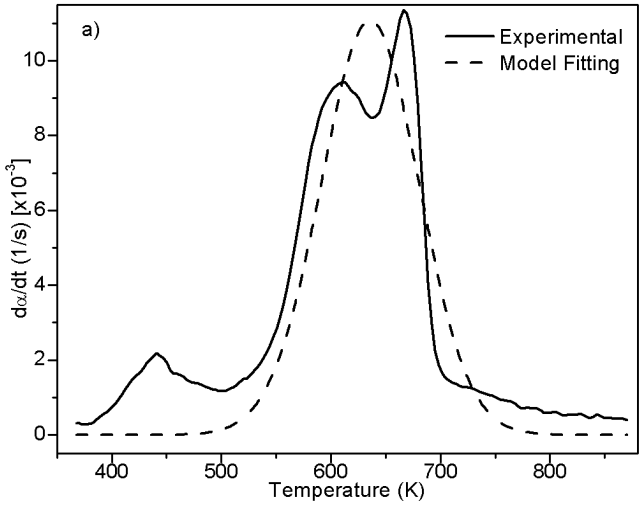

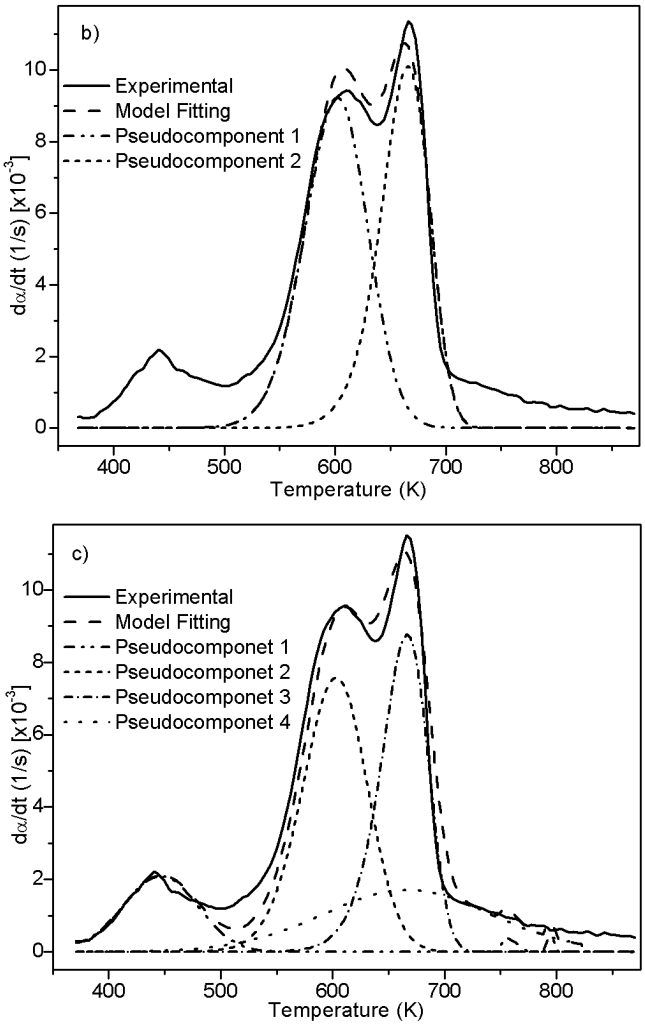

Figure 3. Experimental and fitting of DTG to the DAEM model with different reactions sets for African palm husk pyrolysis at 100K/min
Source: Authors

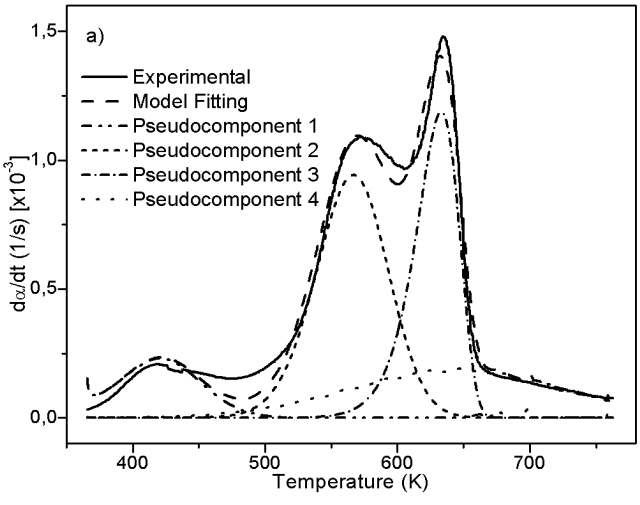

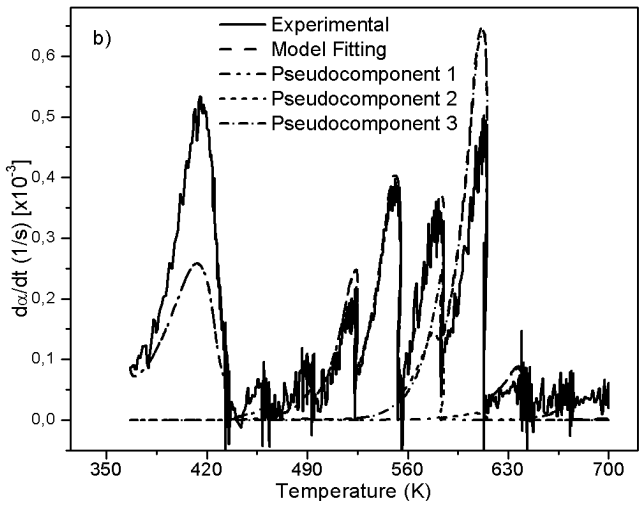

Figure 4. Experimental and fitting of DTG to the DAEM model with different reactions sets for African palm husk pyrolysis at 10 K/min and step heating program.
Source: Authors

Kinetic analysis

The kinetic analysis of pyrolytic process was made between the temperatures that correspond to zone 2 and 3, which can be seen in the Figure 1b. Zone 2 was included because besides is not part of the main pyrolytic event, both zones are overlapped.

Table 1. Fitting parameters of DAEM model with different number of pseudo-components for a heat rate of 100 K/min

	Number of DAEM pseudo-components			
DAEM Parameter	1	2	3	4
c_1	1,575	0,856	0,224	0,228
A_1	1,69E+14	1,79E+14	1,27E+15	1,27E+15
E_{01}	1,88E+05	1,78E+05	1,38E+05	1,38E+05
σ_1	2,43E+04	1,30E+04	1,90E+04	1,90E+04
c_2		0,706	0,858	0,715
A_2		6,09E+14	1,94E+14	1,27E+14
E_{02}		2,03E+05	1,78E+05	1,77E+05
σ_2		6,94E+03	1,31E+04	1,32E+04
c_3			0,704	0,584
A_3			7,03E+14	7,99E+14
E_{03}			2,04E+05	2,04E+05
σ_3			6,98E+03	5,93E+03
c_4				0,403
A_4				1,06E+14
E_{04}				1,95E+05
σ_4				4,38E+04
SE*	0,00133	0,00098	0,0006	0,00055

*SE Standard error of the model
Source: Authors

Figure 1b suggests the use of at least 3 pseudo-components due to the number of peaks. In figure 3, the DAEM model fitting is showed and compared with the experimental data for heat rate of 100 K/min. Considering that the pyrolysis of the biomass used can lead to the production of several chemical species (aromatic polycyclic hydrocarbons, phenolic compounds and oxygenated organic species, the reaction sets and pseudo-components who had the best fitting were selected. In Table 1, the fitting parameters are showed. Reduction of the standard error by increasing the number of pseudo-components is seen. Further analysis was performed using 4 pseudo-components. In Figure 4, results for the fitting of data at 10 K/min heating rate, and 4 pseudo-components for stair function program are presented. Fitting results are shown in Table 1. There is no variation of the parameters of the DAEM model, even for high heating rates.

Values of the parameters of the DAEM model are in the range of previous studies for several biomass, using 3 pseudo-components related to lignin, cellulose and hemicellulose (Cai & Ji, 2007; Cai, Wu, & Liu, 2014; T. Chen, Zhang, & Wu, 2016). Fourth pseudo component is usually associated to oils decomposition. Activation energy for the palm husk is of the same order (Idris, *et al.*, 2010; Yang, *et al.*, 2004).

Mass spectrometry

During the pyrolysis of the palm husk, formation of carbon dioxide (m/z = 44) is detected as result of the thermal decomposition of the cellulose, hemicellulose and lignin. This is one of the products with a complex profile for the pyrolysis of the palm husk. CO_2 is produced also by lignin decarboxylation reactions at high temperature and secondary reactions that occurs in gaseous phase by weak aliphatic bond breaking (Meng, Zhou, Qin, Zhang, & Li, 2013). Methane production (m/z = 12 y 14) at low temperatures is the result of the decomposition of extractive materials and oil that remains in the husk and thermal degradation of hemicellulose and cellulose. Lignin decomposition and production of methane is sustained in all the temperature range, being increased at high temperatures (T. Chen, *et al.*, 2016; Yao, Xu, & Liang, 2016). Relation m/z = 30 is related to the presence of formaldehyde, while m/z = 32 represents the presence of methanol (Malika, Jacques, Fatima, & Mohammed, 2016). Furfural is identified with the relation m/z = 40, while nitrogen compounds are expressed as NO_2 (m/z = 46).

Fitting of DAEM model with 4 pseudo-components is showed in Figure 5 for some of the m/z ratios. In the supplementary material the fitting for all the m/z and heating rates is supplied. Fitting was made with media values of A_j, E_{0j} y σ_j, for each pseudo-component of Table 2. Adjusted parameters were c_j values with 4 pseudo-components for each m/z. Temperature range of the evolved species related with the m/z relations are in agreement with the temperatures of the main pyrolytic event showed in the DTG figures.

Fitting for the m/z = 40 for heating rate of K/min is presented in Figure 5a, a proper fitting is obtained for the model with 4 pseudo-components. Also, evolution of CO_2 is represented

by the same model and number of pseudo-components is represented in Figure 5b. The normalized negative signal for these mass charge relations can be attributed to a higher release of CO_2 before the thermal events (absorbed by the biomass) and the absence of production of this compound at the temperatures of decomposition of oil and extractives. Figures 5c and 5d shows the evolution of m/z = 30 for 100 K/min heating rate, and with stair-like heating program. This relation is related to formaldehyde and shows a good agreement between model and experimental data. Methanol fitting (m/z = 32) was not as good as the previous ones as might be due to production of this compound by decomposition in gaseous phase in secondary reactions.

Table 2. Parameters of DAEM model with four pseudo-components for different heating programs

	Heating Program		
DAEM Parameter	**10 K/min**	**100 K/min**	**Stepheating**
c_1	0,228	0,228	0,186
A_1	1,27E+15	1,27E+15	1,27E+15
E_{01}	1,38E+05	1,38E+05	1,38E+05
σ_1	1,90E+04	1,90E+04	1,90E+04
c_2	0,715	0,715	1,051
A_2	1,27E+14	1,27E+14	1,27E+14
E_{02}	1,77E+05	1,77E+05	1,77E+05
σ_2	1,32E+04	1,32E+04	1,32E+04
c_3	0,584	0,584	0,97
A_3	7,99E+14	7,99E+14	7,99E+14
E_{03}	2,04E+05	2,04E+05	2,04E+05
σ_3	5,93E+03	5,93E+03	5,93E+03
c_4	0,4028	0,4028	0,102
A_4	1,06E+14	1,06E+14	1,06E+14
E_{04}	1,95E+05	1,95E+05	1,95E+05
σ_4	4,38E+04	4,38E+04	4,38E+04
SE*	0,00133	0,00098	0,000057

*SE Standard error of the model
Source: Authors

Table 3 shows the relations m/z of the species produced with high relation intensity/noise, during the heating of the samples that were fitted to DAEM model. In the same way, the evolution of the samples and its evolution with the decomposition of the major components of biomass is showed. Also, a possible source molecule that gives the mass charge relation is proposed according to previous studies (T. Chen, *et al*., 2016; Polat, Apaydin-Varol, & Pütün, 2016; Weerachanchai, Tangsathitkulchai, & Tangsathitkulchai, 2011). During the decomposition of extractives and oil, some relations of m/z related to formaldehyde and CO_2 are weak to been taken account. This is also observed for the NO_2 relation for thermal decomposition of lignin, giving the insight of the non-presence of those compounds for the pyrolysis of extractives and lignin. In the same way, methane, methanol, formaldehyde, furfural, CO_2 and NO_2, are produced in all the range of temperatures that correspond to pyrolysis of cellulose and hemicellulose for all the heating programs.

Table 3. Mass spectrometric intensities selected for kinetic evaluation and its presence in the main thermal events

	m/z	12	14	30	32	40	44	46
Heating Program	Compo-nent/Frag-ment-mole-cule	CH_4	CH_4	Formalde-hyde	Me-thanol	Fur-fural	CO_2	NO_2
10	Extractives	-	+	-	+	+	-	-
	Hemicellu-lose	+	+	+	+	+	+	+
	Cellulose	+	+	+	+	+	+	+
	Lignin	+	+	+	+	+	-	-
100	Extractives	-	+	-	+	+	-	+
	Hemicellu-lose	+	+	+	+	+	+	+
	Cellulose	+	+	+	+	+	+	+
	Lignin	+	+	+	+	+	+	+
step	Extractives	-	-	-	-	-	-	-
	Hemicellu-lose	+	+	+	+	+	-	+
	Cellulose	+	+	+	+	+	+	-
	Lignin	+	+	+	-	+	+	+

Source: Authors

Conclusions

In this study, thermal decomposition of palm husk and fitting to DAEM model was made. Model describes successfully the pyrolytic process kinetics. No change of the kinetic parameters with heating program was observed.

Evolution of m/z ratio of the evolution gas was followed using TG-MS technique. Main molecules found were methane, formaldehyde, furfural, CO_2 and NO_2. For each m/z signal, modeling of the signals with good results for several m/z ratios were obtained. For the signals that did not fit the model can be concluded that its production is also related with secondary reactions in gaseous phase of some of the evolved products. Results of this work could be used to design pyrolysis reactors and, also, as a starting point to optimize them.

Acknowledgements

The present study was financed by Colciencias, project FP44842-281-2015, the Universidad del Atlántico and the Universidad Jorge Tadeo Lozano.

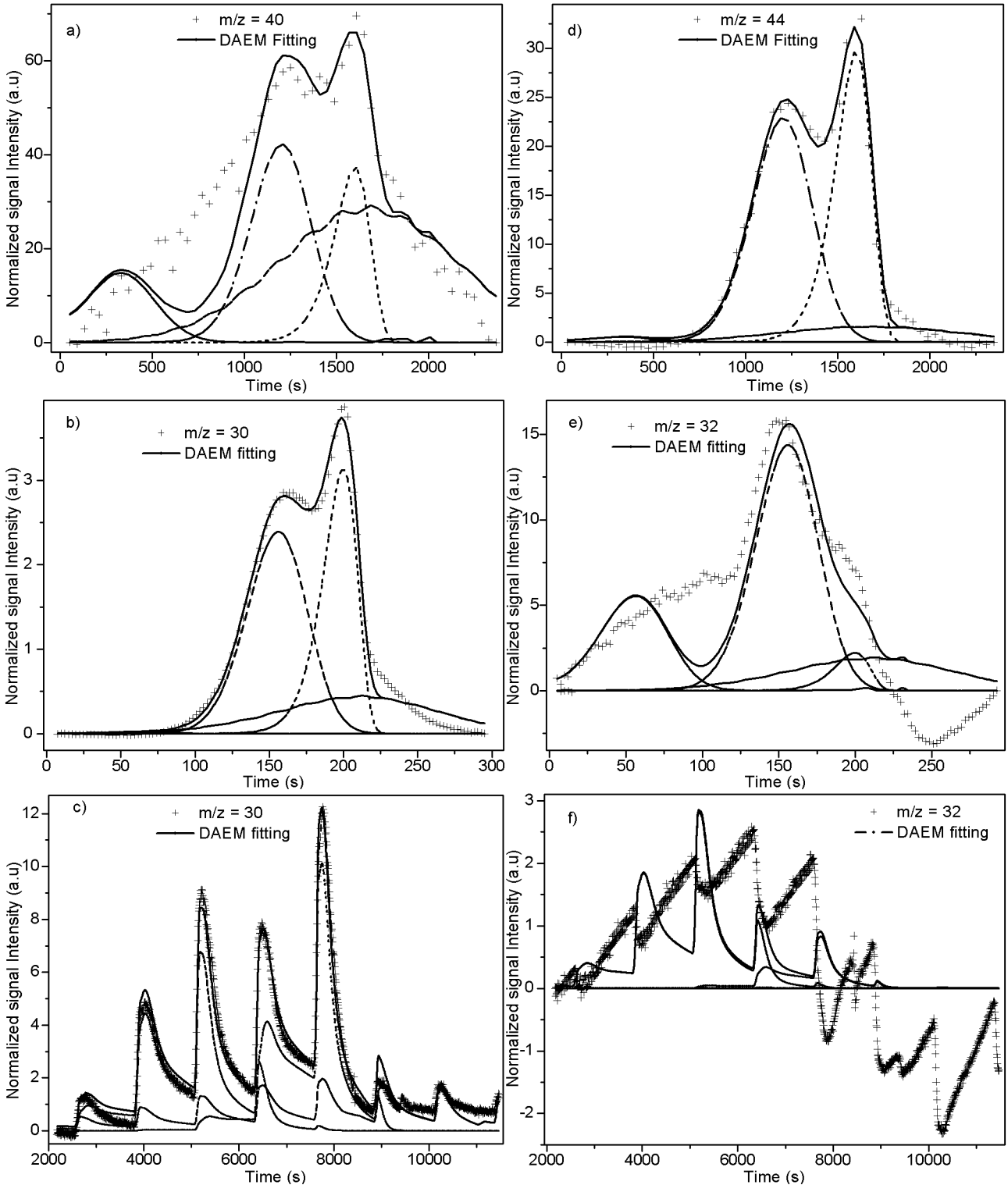

Figure 5. 4 pseudo-components DAEM fitting of selected m/z signal intensities. a) m/z = 40: PKS heated at 10 K/min; b) m/z = 44: PKS heated at 10 K/min; c) m/z = 30: PKS heated at 100 K/min; d) m/z = 32: PKS heated at 100 K/min; d) m/z = 30: PKS heated with stair program; b) m/z = 32: PKS heated with stair program.
Source: Authors

References

Abdelouahed, L., Leveneur, S., Vernieres-Hassimi, L., Balland, L., & Taouk, B. (2017). Comparative investigation for the determination of kinetic parameters for biomass pyrolysis by thermogravimetric analysis. *Journal of Thermal Analysis and Calorimetry*, 1-13.

Abril, A., & Navarro, E. A. (2012). *Etanol a partir de biomasa lignocelulósica*. Valencia: Aleta Ediciones.

Açıkalın, K. (2011). Pyrolytic characteristics and kinetics of pistachio shell by thermogravimetric analysis. *Journal of Thermal Analysis and Calorimetry, 109*(1), 227-235.

Albis, A., Ortiz, E., Suárez, A., & Piñeres, I. (2013). TG/MS study of the thermal devolatization of Copoazú peels (Theobroma grandiflorum). *Journal of thermal analysis and calorimetry*, 1-9.

Caballero, J. A. (1995). *Estudio cinético de la pirólisis de lignina: diseño de un reactor para el estudio de las reacciones secundarias*. Doctor en Ingeniería Química, Universidad de Alicante, Alicante.

Cai, J., & Ji, L. (2007). Pattern search method for determination of DAEM kinetic parameters from nonisothermal TGA data of biomass. *Journal of Mathematical Chemistry, 42*(3), 547-553.

Cai, J., Wu, W., & Liu, R. (2014). An overview of distributed activation energy model and its application in the pyrolysis of lignocellulosic biomass. *Renewable and Sustainable Energy Reviews, 36*(0), 236-246. doi: http://dx.doi.org/10.1016/j.rser.2014.04.052

Camps Michelena, M., & Marcos Martín, F. (2008). *Los biocombustibles*. Madrid Ediciones Mundi-Prensa.

Chen, D., Liu, D., Zhang, H., Chen, Y., & Li, Q. (2015). Bamboo pyrolysis using TG–FTIR and a lab-scale reactor: Analysis of pyrolysis behavior, product properties, and carbon and energy yields. *Fuel, 148*, 79-86.

Chen, N., Ren, J., Ye, Z., Xu, Q., Liu, J., & Sun, S. (2016). Kinetics of coffee industrial residue pyrolysis using distributed activation energy model and components separation of bio-oil by sequencing temperature-raising pyrolysis. *Bioresource technology, 221*, 534-540.

Chen, T., Zhang, J., & Wu, J. (2016). Kinetic and energy production analysis of pyrolysis of lignocellulosic biomass using a three-parallel Gaussian reaction model. *Bioresource Technology, 211*, 502-508.

Cheng, Z., Wu, W., Ji, P., Zhou, X., Liu, R., & Cai, J. (2015). Applicability of Fraser–Suzuki function in kinetic analysis of DAEM processes and lignocellulosic biomass pyrolysis processes. *Journal of Thermal Analysis and Calorimetry, 119*(2), 1429-1438.

Demirbas, A. (2004). Combustion characteristics of different biomass fuels. *Progress in Energy and Combustion Science, 30*(2), 219-230.

Donskoi, E., & McElwain, D. (2000). Optimization of coal pyrolysis modeling. *Combustion and flame, 122*(3), 359-367.

Gani, A., & Naruse, I. (2007). Effect of cellulose and lignin content on pyrolysis and combustion characteristics for several types of biomass. *Renewable energy, 32*(4), 649-661.

Gottipati, R., & Mishra, S. (2011). A kinetic study on pyrolysis and combustion characteristics of oil cakes: Effect of cellulose and lignin content. *Journal of fuel chemistry and technology, 39*(4), 265-270.

Idris, S. S., Rahman, N. A., Ismail, K., Alias, A. B., Rashid, Z. A., & Aris, M. J. (2010). Investigation on thermochemical behaviour of low rank Malaysian coal, oil palm biomass and their blends during pyrolysis via thermogravimetric analysis (TGA). *Bioresource Technology, 101*(12), 4584-4592.

Janković, B. (2014). The pyrolysis process of wood biomass samples under isothermal experimental conditions—energy density considerations: application of the distributed apparent activation energy model with a mixture of distribution functions. *Cellulose, 21*(4), 2285-2314.

Khelfa, A., Bensakhria, A., & Weber, J. (2013). Investigations into the pyrolytic behaviour of birch wood and its main components: primary degradation mechanisms, additivity and metallic salt effects. *Journal of Analytical and Applied Pyrolysis, 101*, 111-121.

Lv, D., Xu, M., Liu, X., Zhan, Z., Li, Z., & Yao, H. (2010). Effect of cellulose, lignin, alkali and alkaline earth metallic species on biomass pyrolysis and gasification. *Fuel Processing Technology, 91*(8), 903-909.

Malika, A., Jacques, N., Fatima, B., & Mohammed, A. (2016). Pyrolysis investigation of food wastes by TG-MS-DSC technique. *Biomass Conversion and Biorefinery, 6*(2), 161-172.

Meng, A., Zhou, H., Qin, L., Zhang, Y., & Li, Q. (2013). Quantitative and kinetic TG-FTIR investigation on three kinds of biomass pyrolysis. *Journal of Analytical and Applied Pyrolysis, 104*, 28-37.

Montiel, J. L. R. (2003). La biomasa cañera como alternativa para el incremento de la eficiencia energética y la reducción de la contaminación ambiental. *Centro Azúcar, 30*(2), 14-21.

Oseghale, S. D., Mohamed, A. F., & Chikere, A. O. (2017). Status Evaluation of Palm Oil Waste Management Sustainability in Malaysia.

Perdices, M. B. (2009). La Biomasa como Recurso Energético. In P. Ramos Castellanos (Ed.), *Cambio Climático, ¿Un desafío a nuestro alcance?* (pp. 167-180). Salamanca: Ediciones Universidad de Salamanca.

Polat, S., Apaydin-Varol, E., & Pütün, A. E. (2016). Thermal decomposition behavior of tobacco stem Part I: TGA–FTIR–MS analysis. *Energy Sources, Part A: Recovery, Utilization, and Environmental Effects, 38*(20), 3065-3072.

Rodríguez, R. P., Sierens, R., Verhelst, S., & Frontela, N. F. (2008). Evaluación del funcionamiento de motores de combustión interna trabajando con biodiesel. *Ingeniería Mecánica, 3*, 33-38.

Soto, N. A., Machado, W. R., & López, D. L. (2010). Determinación de los parámetros cinéticos en la pirólisis del pino ciprés. *Quim. Nova, 33*(7), 1500-1505.

Várhegyi, G. (2007). Aims and methods in non-isothermal reaction kinetics. *Journal of Analytical and Applied Pyrolysis, 79*(1), 278-288.

Várhegyi, G., Szabó, P., & Antal, M. J. (2002). Kinetics of charcoal devolatilization. *Energy & fuels, 16*(3), 724-731.

Wang, S., Guo, X., Wang, K., & Luo, Z. (2011). Influence of the interaction of components on the pyrolysis behavior of biomass. *Journal of Analytical and Applied Pyrolysis, 91*(1), 183-189.

Weerachanchai, P., Tangsathitkulchai, C., & Tangsathitkulchai, M. (2011). Characterization of products from slow pyrolysis of palm kernel cake and cassava pulp residue. *Korean Journal of Chemical Engineering, 28*(12), 2262-2274.

Yang, H., Yan, R., Chen, H., Lee, D. H., & Zheng, C. (2007). Characteristics of hemicellulose, cellulose and lignin pyrolysis. *Fuel, 86*(12), 1781-1788.

Yang, H., Yan, R., Chin, T., Liang, D. T., Chen, H., & Zheng, C. (2004). Thermogravimetric analysis– Fourier transform infrared analysis of palm oil waste pyrolysis. *Energy & fuels, 18*(6), 1814-1821.

Yao, X., Xu, K., & Liang, Y. (2016). Analytical Pyrolysis Study of Peanut Shells using TG-MS Technique and Characterization for the Waste Peanut Shell Ash. *Journal of Residuals Science & Technology, 13*(4).